

# Harmonic reduction in power grids: implementing a four-legged multilevel inverter as an active power filter using model predictive control

Asep Andang<sup>1</sup>, Firmansyah Maulana Nursuwars<sup>2</sup>, Andri Ulus Rahayu<sup>1</sup>, Imam Taufiqurrahman<sup>1</sup>,  
Ervan Paryono<sup>1</sup>

<sup>1</sup>Department of Electrical Engineering, Faculty of Engineering, Universitas Siliwangi, Tasikmalaya, Indonesia

<sup>2</sup>Department of Informatics, Faculty of Engineering, Universitas Siliwangi, Tasikmalaya, Indonesia

## Article Info

### Article history:

Received Aug 5, 2024

Revised Mar 12, 2025

Accepted Mar 29, 2025

### Keywords:

Active power filter

Four-leg multilevel inverter

Grid connected converter

Harmonics reduction

Model predictive control

## ABSTRACT

This study explores the implementation of a five-level cascaded three-phase four-wire inverter as an active power filter to mitigate harmonics in power grids. Harmonic components in the load current are transformed and filtered to create a reference current, which serves as the foundation for designing the inverter's switching pattern. The predicted current, generated through circuit modeling, is compared with the reference current using the model predictive control (MPC) method. The accuracy of this approach is evaluated using a cost function that measures the difference between the predicted and reference currents. Simulation results reveal that the application of the hybrid power filter can effectively suppress harmonics, reducing the total harmonic distortion (THD) to below 5%, thereby meeting power quality standards. Furthermore, it addresses load imbalances, ensuring that the phase currents at the source remain nearly equal. Additionally, the hybrid power filter significantly decreases the neutral current, reducing it to just one-tenth of its original value. While MPC has demonstrated its effectiveness in controlling power converters and multilevel inverters, its application to active power filters remains underexplored. This study investigates the potential of a four-legged multilevel inverter with MPC to enhance power quality by reducing harmonics in three-phase four-wire systems.

*This is an open access article under the [CC BY-SA](#) license.*



## Corresponding Author:

Asep Andang

Department of Electrical Engineering, Faculty of Engineering, Universitas Siliwangi

St. Siliwangi No.24, Tasikmalaya 46115, Indonesia

Email: andhangs@unsil.ac.id

## 1. INTRODUCTION

The electrical power used in household, office, industrial, commercial, transportation, aviation, military, and utility systems today relies on power electronics technology [1]. Power electronics technology can make the system simpler and more compact [2], resulting in high efficiency [3], and more reliable accuracy [4], [5]. The use of semiconductor components in power electronics technology for various equipment is inseparable from the switching of electrical parameters, either current or voltage. The switching process in the converter circuit produces pollution from the power-supply source. This semiconductor switch produces a follow-up wave with a frequency multiple of the initial power supply frequency. Waves with frequencies that correlate with the source frequency are known as harmonics [6]. This harmonic distorts the fundamental waves such that the power supply waves become damaged and do not become purely sinusoidal. The magnitude of

damage to the power supply wave due to harmonics can be determined using the total harmonic distortion (THD), which is in the form of a comparison of the total wave with the frequency of generation to the size of the fundamental part [7].

If an electrical grid has a large harmonic, then the influence on the conductor causes the Joule effect losses [8], and in transformers, it causes an increase in copper and core losses [9]. Harmonic currents in generators can increase hysteresis, eddy currents, and core losses [10]. In electric motors, the presence of harmonics decreases torque [11]. Harmonics in electrical grid protection equipment result in malfunctions in circuit breakers, fuses [12], protection relays [13], and control systems. In communication systems, they can interfere with communication signals [14].

Harmonic reduction began with the discovery of harmonic waves in the network. Initially performed using a passive power filter, this method is inexpensive, but only works on static loads and is unreliable with dynamic loads [15]. The implementation of power electronics has led to active power filters that are widely used in networks with dynamic loads from small to large [16]. These filters can reduce the harmonics caused by networked converters. The converter generates harmonic waves in opposite phases, without fundamental waves. When added to the point of common coupling (PCC), it eliminates harmonic waves caused by nonlinear loads [17]. When generating this opposite-phase harmonic wave, the converter in the active power filter requires a reference wave to generate a predicted wave for harmonic reduction. This reference wave is formed from the extraction of load harmonic waves by various methods, including instantaneous reactive power theory (IRPT) [18] by utilizing the reactance power of PQ, and then modifying IRPT [19] using synchronous reference frame (SRF) [20] by transforming the three-phase system of abc into dq using the Clark and Park transformations. This extraction method produces waves that are used as references to generate the opposite-phase harmonic signals.

The converters used in active power filters vary depending on the configuration of the power grid, that is, single-phase converters, three-phase three-wire converters, and four-wire three-phase converters. Single-phase converters are used when the harmonics to be reduced are present in a single-phase load. In contrast, three-phase three-wire converters are used in three-phase systems with three-phase loads or loads by applying a phase-to-phase voltage. The use of the four-wire three-phase converter is wider, covering a single-phase load, three-wire three-phase load, and four-wire three-phase load.

Multilevel inverters offer a lower THD owing to their higher voltage levels, which are close to the desired sinusoidal signal in AC waves [21]. However, the more levels that are generated, the more semiconductor components that are used, and the more complex the existing switching methods will be [22], which will encourage a potential fault in the switch, so that protection is needed to prevent it [23]. Various control strategies for active power filters have been proposed in literature. Anssari *et al.* [24] introduced an adaptive sliding mode control (SMC) for PV systems to mitigate chattering phenomena and high-frequency oscillations affecting traditional SMC. They proposed a particle swarm optimization (PSO) algorithm to fine-tune the SMC gains, specifically to control the variable step of the standard perturb and observe (P&O) algorithm. Sundaram *et al.* [25] improved the proportional-integral (PI) controller tuning for shunt active power filter (SAPF) in systems with complex, dynamic, and nonlinear loads using a genetic algorithm (GA) and novel queen bee assisted GA (QBGA) to achieve optimal gain values, ensuring the rapid generation of compensating currents with minimal errors to nullify harmonic currents. Saad and Zellouma [26] enhanced three-level inverters used as shunt APF by leveraging advantages of multilevel inverters. They introduced a fuzzy logic controller for harmonic currents and inverter DC voltage, addressing the limitations of traditional two-level APFs. Badra *et al.* [27] proposed a backstepping control strategy for a three-level four-leg SAPF system to enhance the power quality by compensating harmonics and zero-sequence currents while achieving a unity power factor. Monroy-Morales *et al.* [28] validated a new active power filter (APF) prototype based on a three-phase, three-level neutral point clamped (NPC) inverter, designed to enhance power quality through selective harmonic and reactive power compensation. They implemented a three-dimensional space vector modulator (3D-SVPWM) technique to generate precise compensation currents. Mehraza *et al.* [29] proposed a direct Lyapunov-based control technique for active power filtering to enhance power quality and achieve a unity power factor. It compensates for the harmonic current components and reactive power caused by nonlinear grid-connected loads while ensuring seamless integration through multilevel converter topologies. In addition, intelligence-based control techniques have been introduced to stabilize active power filters, such as artificial neural network (ANN) [30], recurrent neural network (RNN) [31], deep learning [32], and long short-term memory (LSTM) [33].

Several discussions related to MPC in active power filters have been widely conducted by various researchers. Sahli *et al.* [34] proposed a modified packed U-cell five-level inverter (MPUC5) with an MPC strategy for single-phase APF applications and to eliminate harmonic currents and compensate reactive power at the PCC, addressing the issues caused by local non-linear loads connected to the grid. Adam *et al.* [35] develop a finite control set MPC technique for controlling voltage source inverters (VSIs) in APF and to enhance harmonic current mitigation and eliminate asymmetrical loads in power distribution networks affected by

nonlinear loads, distributed generation, and renewable energy sources. Skjong *et al.* [36] evaluated a distributed control hierarchy with real-time MPC implementation for dynamic systems, specifically focusing on harmonic mitigation in power systems and addressing the challenges associated with implementing MPC in fast dynamic systems, including high computational loads and limited flexibility in embedded devices. However, the development of this method for active power filters remains open. With more advanced embedded technology, the iteration process required for MPC will be easier. To the best of our knowledge, the use of multilevel inverters as active power filters in the MPC method is still very limited.

The main problem addressed is the reduction of harmonic distortion in three-phase, four-wire power grids, which is critical for maintaining power quality. Harmonics from nonlinear loads and power electronic converters cause issues such as increased losses, equipment overheating, and malfunctioning of protective devices. Conventional passive filters are limited to static load conditions and fail to adapt dynamically. While more effective, active power filters require precise current reference generation and advanced control strategies. This study focused on the implementation of a five-level multilevel inverter as a hybrid active power filter controlled by MPC. The challenge is to develop an efficient and adaptive control mechanism to minimize THD and address load imbalances while ensuring a robust and scalable solution for complex power systems.

The main contributions and novelty of this study are as follows: i) This paper presents a hybrid power filter based on a five-level multilevel inverter using MPC to reduce harmonic distortions in a three-phase, four-wire power grid. The simulation results show its capability to lower the THD below 5%, meeting power quality standards. ii) The proposed system reduces harmonic currents and addresses load imbalances, thereby significantly reducing the neutral current by up to one-tenth of its original value. This feature improves the stability and efficiency of the power distribution systems. iii) This study explored MPC for active power-filter applications in multilevel inverters, an area with limited research. This advances the understanding of MPC effectiveness in improving the power quality and balancing loads in complex power systems.

This paper is organized into several sections to systematically demonstrate its contributions and relevance. Section 1 introduces the significance of power electronics in various applications and the challenges posed by harmonic distortions in power grids, emphasizing the novelty of using a five-level multilevel inverter with an MPC to address these issues. Section 2 reviews existing harmonic mitigation techniques, highlighting the limitations of passive filters and traditional active filters, while identifying research gaps in applying MPC to hybrid power filters. Section 3 describes the research methodology, details the hybrid active power filter design, the use of SRF theory for reference current generation, and the implementation of MPC for optimizing inverter switching patterns to reduce harmonic distortion. Section 4 presents the simulation results, demonstrating the effectiveness of the proposed system in reducing the THD below 5%, balancing loads, and minimizing neutral currents under both balanced and unbalanced load conditions, with a discussion comparing it to conventional methods. Finally, section 5 concludes the paper, summarizes the achievements, and suggests future directions.

## 2. METHOD

A three-phase, four-wire power grid circuit connected by a nonlinear load generated a harmonic current. This circuit was then connected to a serial-mounted passive power filter with an active power filter at the point of common coupling (PCC). It has an active power filter in the form of a three-phase, four-wire, multistage converter network. Current and voltage sensors are processed using the SRF method to generate the reference current used in the MPC method. The full range of these networks is illustrated in Figure 1. The simulated network was a three-phase, four-wire voltage network that accommodated the presence of a single-phase load connected to a three-phase network. These single-phase loads affect the load balance. The magnitude of this load imbalance affected the magnitude of the neutral current.

### 2.1. Multilevel converter

A clamped diode cascade converter is a multilevel inverter that produces an output voltage with a low harmonic distortion (low THD). This inverter uses a combination of semiconductor switches and supporting components to produce output voltage levels approaching sinusoidal waveforms. This converter has four semiconductor switches clamped with a diode on each arm. The four arms consisted of phases a, b, c, and neutral, as shown in Figure 2. For the power supply supplied by  $V_{dc}$ , the voltage is equal to the use of  $C_1$  and  $C_2$  with the same value, such that  $V_{C1} = V_{C2}$  is ideal.

There were four IGBTs in each arm:  $S_{1a}$ ,  $S_{2a}$ ,  $S'_{1a}$ , and  $S'_{2a}$ .  $S_{1a}$  and  $S'_{1a}$  are negative with each other, and so are  $S_{2a}$  and  $S'_{2a}$ , so if  $S_{1a}$  has a value of "1" then  $S'_{1a}$  has a value of "0" and if  $S_{2a}$  has a value of "0" then  $S'_{2a}$  has a value of "1." From the combination of each arm,  $3^4 = 81$  possible switches were produced. The three possibilities for each arm are listed in Table 1.

From Table 1, two levels of positive voltage can be adjusted, plus two levels of negative voltage, so that five levels of voltage with zero are obtained at this level. When switching conditions  $S_{1a}$  and  $S_{2a}$  are on, a voltage of  $V_{dc}$  is produced, which is measured between phases a and N. When  $S_{2a}$  is on,  $V_{C2}$  will be measured between phases a and N, and if  $S_{1a}$  and  $S_{2a}$  are off, the voltage value of phases a to N will be zero.

The voltage generated from phase x to point N depends on the switching signal of each IGBT in each arm; this can be seen from (1) [37].

$$\begin{bmatrix} v_{aN} \\ v_{bN} \\ v_{cN} \\ v_{dN} \end{bmatrix} = v_{C1} \begin{bmatrix} S_{a1} \\ S_{b1} \\ S_{c1} \\ S_{n1} \end{bmatrix} + v_{C2} \begin{bmatrix} S_{a2} \\ S_{b2} \\ S_{c2} \\ S_{n2} \end{bmatrix} \quad (1)$$

While the phase voltage x to point n is generated from (2).

$$\begin{bmatrix} v_{an} \\ v_{bn} \\ v_{cn} \end{bmatrix} = v_{C1} \begin{bmatrix} S_{a1} - S_{n1} \\ S_{b1} - S_{n1} \\ S_{c1} - S_{n1} \end{bmatrix} + v_{C2} \begin{bmatrix} S_{a2} - S_{n2} \\ S_{b2} - S_{n2} \\ S_{c2} - S_{n2} \end{bmatrix} \quad (2)$$

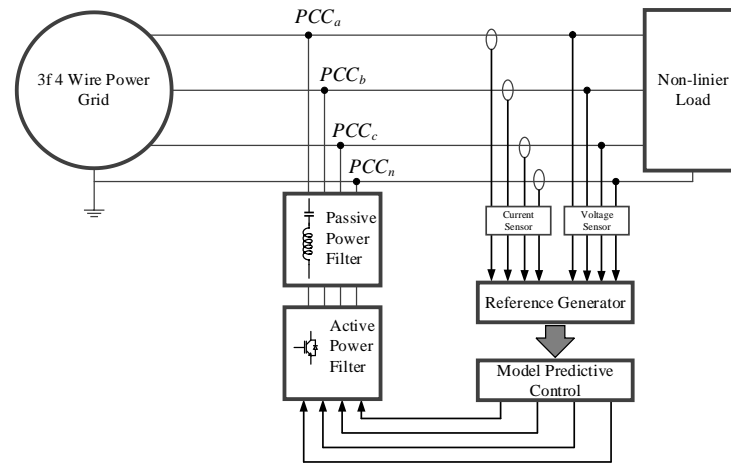


Figure 1. Power grid-connected nonlinear loads with active power filters

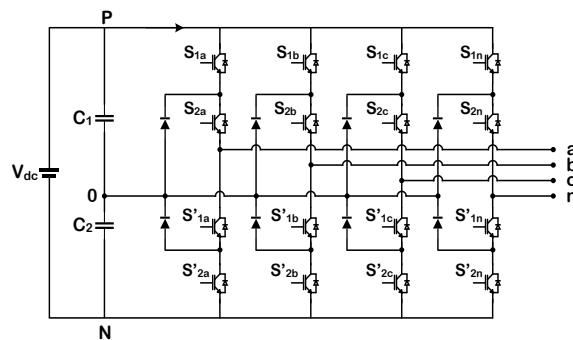


Figure 2. Network of three-phase, four-wire multilevel converter

Table 1. Switching state of multilevel converter

Switching signal				Output voltage
$S_{1x}$	$S_{2x}$	$S'_{1x}$	$S'_{2x}$	$V_{xN}$
'1'	'1'	'0'	'0'	$V_{C1} + V_{C2}$
'0'	'1'	'1'	'0'	$V_{C2}$
'0'	'0'	'1'	'1'	0

## 2.2. Reference current generation

The synchronous reference frame (SRF) theory is employed to transform three-phase currents ( $i_a$ ,  $i_b$ ,  $i_c$ ) into a rotating reference frame ( $dq0$ ) using Clark and Park transformations. This transformation simplifies the analysis and control of three-phase systems by converting the sinusoidal waveforms into DC components in the  $dq0$  domain. The process begins with the Clark transformation, which projects three-phase currents into a two-phase stationary reference frame ( $\alpha\beta$ ). This was achieved by using the following equation:

$$\begin{bmatrix} i_\alpha \\ i_\beta \end{bmatrix} = \begin{bmatrix} 1 & -\frac{1}{2} & -\frac{1}{2} \\ 0 & \frac{\sqrt{3}}{2} & -\frac{\sqrt{3}}{2} \end{bmatrix} \begin{bmatrix} i_a \\ i_b \\ i_c \end{bmatrix}$$

where  $i_\alpha$  and  $i_\beta$  represent the two orthogonal components of the three-phase current in the stationary reference frame.

Once the currents are in the  $\alpha\beta$  frame, the Park transformation is applied to rotate this stationary frame to align it with the synchronous reference frame ( $dq$ ). This alignment is achieved by utilizing the system's instantaneous angular position ( $\theta$ ) to project the currents onto the rotating  $dq$ -axis using:

$$\begin{bmatrix} i_d \\ i_q \end{bmatrix} = \begin{bmatrix} \cos\theta & \sin\theta \\ -\sin\theta & \cos\theta \end{bmatrix} \begin{bmatrix} i_\alpha \\ i_\beta \end{bmatrix}$$

here,  $i_d$  represents the direct axis component, which aligns with the system voltage, and  $i_q$  represents the quadrature axis component orthogonal to  $i_d$ . These components are now DC signals, making them easier to filter and process for control.

The final step is to generate the reference currents by filtering the  $i_d$  and  $i_q$  components using a low-pass filter to remove harmonic distortion. The filtered  $i_{d(ref)}$  component is further corrected using a DC regulator, while the  $i_q$  and  $i_0$  components are transformed back to the three-phase  $abc$  domain via inverse Park and Clark transformations. These reference currents ( $i_{a(ref)}$ ,  $i_{b(ref)}$ ,  $i_{c(ref)}$ ) guide the inverter switching patterns to inject compensating currents, ensuring harmonic reduction and a balanced system operation.

The reference currents to be used in the MPC method were generated using the synchronous reference frame (SRF) theory. The decomposition diagram blocks to generate the reference currents  $i_{a(ref)}$ ,  $i_{b(ref)}$ , and  $i_{c(ref)}$  are shown in Figure 3. The change of phase current  $abc$  to  $dq$  current is done using (3).

$$\begin{bmatrix} i_d \\ i_q \\ i_0 \end{bmatrix} = \frac{2}{3} \begin{bmatrix} \sin(\omega t) & \sin(\omega t - \frac{2\pi}{3}) & \sin(\omega t + \frac{2\pi}{3}) \\ \cos(\omega t) & \cos(\omega t - \frac{2\pi}{3}) & \cos(\omega t + \frac{2\pi}{3}) \\ \frac{1}{2} & \frac{1}{2} & \frac{1}{2} \end{bmatrix} \begin{bmatrix} i_a \\ i_b \\ i_c \end{bmatrix} \quad (3)$$

The  $i_{d(ref)}$  current was obtained via  $i_d$  filtering using a low-pass filter and correction from the DC regulator. The currents  $i_{q(ref)}$  and  $i_{0(ref)}$  are generated by converting by -1 of  $i_q$  and  $i_0$ . It was then converted again to generate the reference currents  $i_{a(ref)}$ ,  $i_{b(ref)}$ , and  $i_{c(ref)}$  using (4).

$$\begin{bmatrix} i_{a(ref)} \\ i_{b(ref)} \\ i_{c(ref)} \end{bmatrix} = \begin{bmatrix} \sin(\omega t) & \cos(\omega t) & 1 \\ \sin(\omega t - \frac{2\pi}{3}) & \cos(\omega t - \frac{2\pi}{3}) & 1 \\ \sin(\omega t + \frac{2\pi}{3}) & \cos(\omega t + \frac{2\pi}{3}) & 1 \end{bmatrix} \begin{bmatrix} i_{d(ref)} \\ i_{q(ref)} \\ i_{0(ref)} \end{bmatrix} \quad (4)$$

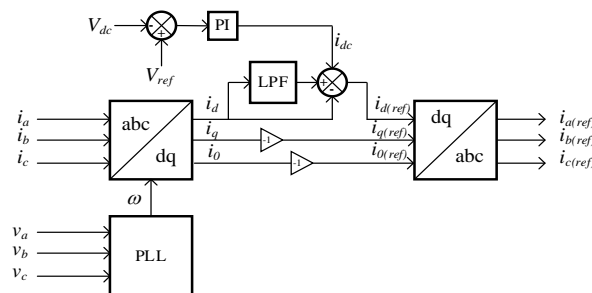


Figure 3. The method reference currents were generated using the SRF method

### 2.3. Model predictive control

The MPC is chosen for generating optimal switching patterns in multilevel inverters because of its ability to predict future currents  $i(k+1)$  based on the system parameters and applied switching states. By leveraging a cost function  $g = |i_{ref} - i(k+1)|$ , the MPC minimizes the difference between the reference current ( $i_{ref}$ ) and predicted current, effectively reducing THD and enhancing power quality. Its flexibility allows it to adapt to dynamic and unbalanced load conditions, ensuring consistent performance in three-phase four-wire systems. Furthermore, MPC's computational efficiency of MPC, enabled by advancements in embedded technologies, makes it practical for real-time applications. The capability of the algorithm to handle multilevel switching with numerous combinations (e.g., 81 for a five-level inverter) ensures an optimal voltage output while maintaining precision. These advantages make MPC an ideal choice for improving control accuracy and reliability in multilevel inverter applications.

The MPC algorithm used in this study is as follows:

- Initialize parameters  
The initial value of  $i(k)$  (current at time  $k$ ) is set. We define the network parameters, including  $R$ ,  $L$ ,  $C$ , and the sampling time  $T_s$ .
- Calculate reference current  
Transform the three-phase current ( $i_a$ ,  $i_b$ ,  $i_c$ ) into the  $dq0$  domain using Clark and Park transformations as in (5):

$$\begin{bmatrix} i_d \\ i_q \\ i_0 \end{bmatrix} = T \begin{bmatrix} i_a \\ i_b \\ i_c \end{bmatrix} \quad (5)$$

apply a low-pass filter to  $i_d$  to remove harmonic components and generate the reference current ( $i_{ref}$ ).

- Predict future current  
Use the system equation (based on electrical circuit dynamics) as shown in (6).

$$i(k+1) = i(k) + T_s \left( \frac{v_{pcc} - v_{inv} - R \cdot i(k)}{L} \right) \quad (6)$$

Current  $i(k+1)$  is predicted using inverter voltage ( $v_{inv}$ ).

- Evaluate cost function  
Compute the cost function ( $g$ ) as the absolute difference between the predicted current  $i(k+1)$  and the reference current ( $i_{ref}$ ), as shown in (7).

$$g = |i_{ref} - i(k+1)| \quad (7)$$

- Optimize switching pattern  
Iterate all 81 possible switching combinations for the multilevel inverter. Select the switching pattern that minimizes  $g$ .
- Generate switching signal  
The optimal switching pattern is applied to the inverter to produce the desired voltage ( $v_{inv}$ ).
- Repeat the process  
Update  $i(k)$  with the predicted value  $i(k+1)$ . Step 3 is continued for the next sampling period.

To generate a switching signal with the MPC method, a reference current derived from harmonic signal extraction, as shown in (4), and a predicted current signal are required. The predicted current is built from the equation of the system series in the form of a closed loop, as shown in (8).

$$v_{pccx} = L \frac{di}{dt} + R \cdot i + \frac{1}{C} \int i dt + v_{inv} \quad (8)$$

Where  $v_{pccx}$  is the voltage at the point of common coupling phase  $x$ ,  $L$ ,  $R$ , and  $C$  are the values of resistance, inductance, and capacitance of the passive power filter, respectively, and  $v_{inv}$  is the value of the inverter voltage according to (2) from phase  $x$  to  $n$  or according to (9).

$$v_{inv} = v_{xn} \quad (9)$$

The next process is to discretize (8), both derivatives and integrals, using forward Euler so that the prediction current used in the switching process is obtained as in (10).

$$i(k+1) = \frac{1}{\left(\frac{L}{T_s} + R + \frac{T_s}{C}\right)} \left( v_{pccx} - v_{inv} - \left( \frac{T_s}{C} - \frac{L}{T_s} \right) (i(k)) \right) \quad (10)$$

Where  $i(k+1)$  is the prediction flow using the MPC method.  $T_s$  is the time sampling and  $i(k)$  is the extrapolation current at time  $k$ . To determine the best switching pattern such that the predicted current is the same as the reference current, the cost function is used, which is the absolute value of the difference between the reference current and the reference current, as in (11). In one sampling time, 81 iterations were performed to obtain the smallest  $g$ -value. This smallest  $G$  produces a prediction value that is the result of switching, according to (2).

$$g = |i_{a(ref)} - i_a(k+1)| + |i_{b(ref)} - i_b(k+1)| + |i_{c(ref)} - i_c(k+1)| + |i_n(ref) - i_n(k+1)| \quad (11)$$

### 3. RESULTS AND DISCUSSION

The model was tested by simulating the circuits and equations using MATLAB Simulink. The simulation had three main parts: a plant with a three-phase, four-wire source connected to a nonlinear load; reference current generation using SRF derived from load currents and voltages; and a hybrid power filter comprising an LC passive filter and an active filter as a three-phase four-wire converter. Simulink was used to simulate the circuit for the basic parameters described in MATLAB. MPC programming is performed using (10), where  $i(k+1)$  is the predicted current obtained from the inverter voltage  $v_{inv}$  from (2). The predicted current must be close to the reference current to reduce harmony, as determined using the cost function in (11). To assess the performance of the model, tests were conducted using balanced and unbalanced nonlinear loads.

#### 3.1. Balanced load simulation

The balanced load test was performed by connecting a three-phase, four-wire electrical network with a single-phase rectifier connected to the resistive load  $R$  and an inductor  $L$  with a value of  $R_a = R_b = R_c = 25 \Omega$  while the inductor value is 70 mH. The load circuit is illustrated in Figure 4. Simulations are performed to assess the performance of the hybrid power filter when subjected to nonlinear loads. Figure 5(a) illustrates the load current, which shows significant distortion, whereas Figure 5(b) depicts the corresponding load voltage. The presence of harmonic distortion causes the load current to deviate from the ideal sinusoidal waveform. Specifically, the THD of the load current was measured to be 32.34%, as shown in Figure 5(c), whereas the load voltage exhibited a THD of 3.11%, as shown in Figure 5(d).

The load current, which contained harmonic distortion, as shown in Figure 6(a), was analyzed and processed using the SRF method, as outlined in Figure 3. This process begins with the Clark transformation, which converts three-phase currents ( $abc$ ) into a two-phase stationary reference frame ( $dq0$ ), producing the signal depicted in Figure 6(b). The resulting  $dq0$  signal was then passed through a low-pass filter to remove high-frequency harmonics, yielding a smoothed reference current in the  $dq0$  domain, as shown in Figure 6(c). Finally, the reference current in the  $dq0$  domain is retransformed back into the three-phase  $abc$  reference frame using inverse Clark transformation. This retransformation, illustrated in Figure 6(d), provides the reference currents required to guide the switching patterns of the inverter for effective harmonic compensation and load balancing.

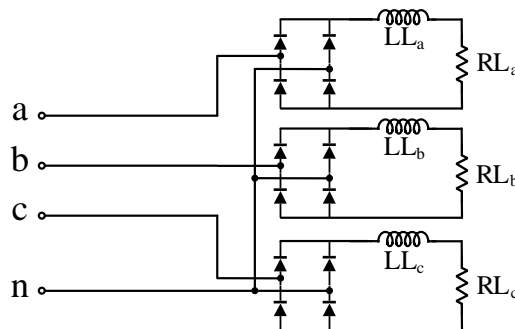


Figure 4. Load circuit

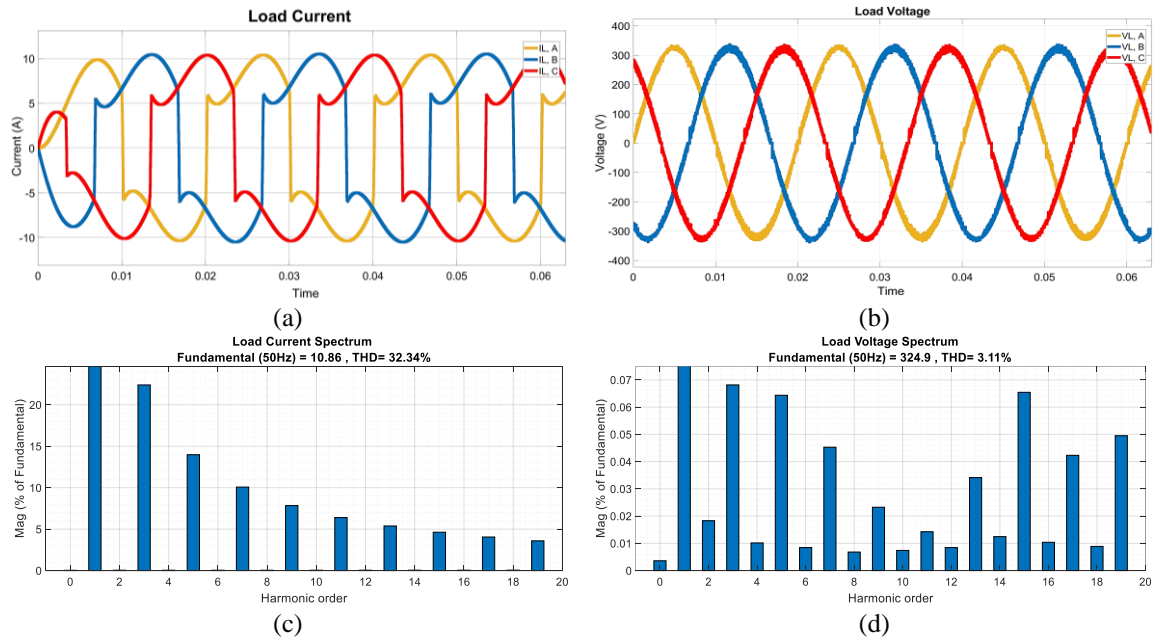


Figure 5. Current waveform and voltage: (a) load current, (b) load voltage, (c) THD current, and (d) THD load voltage

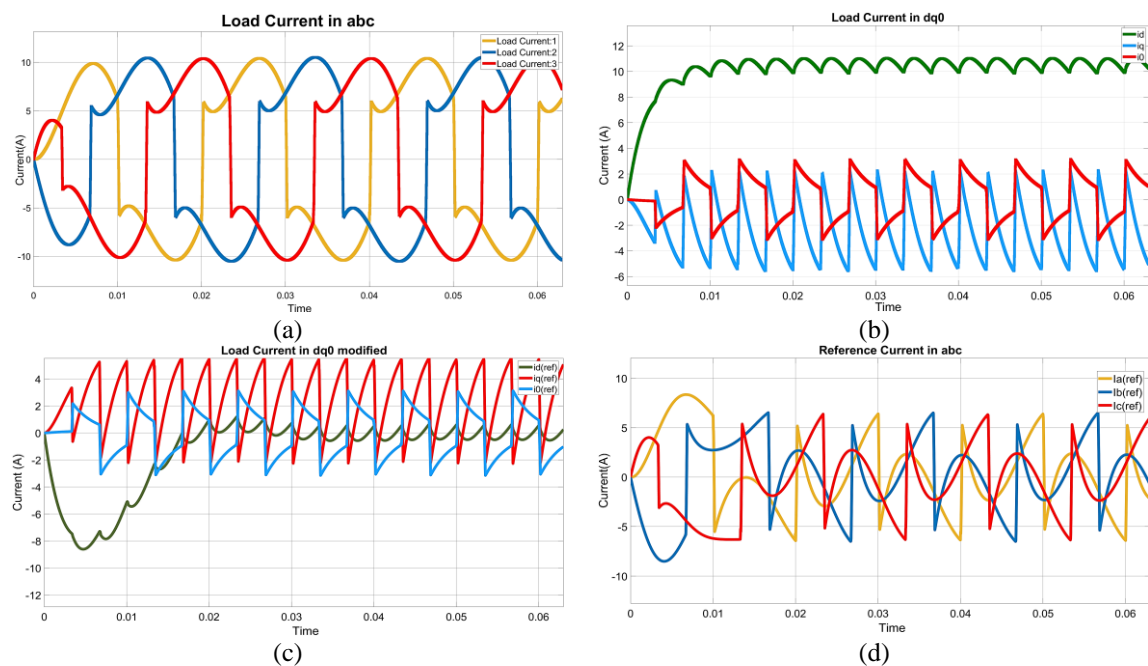


Figure 6. Current waveform: (a) load current in abc, (b) load current in dq0, (c) reference current in dq0, and (d) reference current in abc

The injection of compensating currents by the converter voltage at the PCC effectively reduced the current drawn from the source, thereby decreasing the harmonic content of the source current. This reduction in harmonics was confirmed by the observed decrease in THD of the source current. Figure 7(a) illustrates the source current waveform, whereas Figure 7(b) depicts the corresponding source voltage waveform. The THD values for the source current and voltage are presented in Figures 7(c) and 7(d), respectively, highlighting the improved power quality achieved by the hybrid power filter. In addition, the installation of the hybrid power filter significantly reduced the neutral current. Before filter installation, the neutral current at the load averages 5.5 amperes; after the filter is applied, the neutral current at the source decreases to



approximately 0.8 amperes. This reduction underscores the effectiveness of the filter in balancing the load and mitigating the effect of harmonic distortions on the power system.

Under balanced load conditions, harmonic current generation was consistent across the phases, with no notable discrepancies. In the SRF, the ripples in the  $i_d$  current are attributed to harmonic distortion. The simulation demonstrated the connection between harmonic currents and the increased neutral current. Implementing a harmonic power filter effectively reduces the THD in the current of each phase, ensuring a balanced reduction. In addition, the hybrid power filter significantly decreased the neutral current, leaving only minor spikes caused by the MPC algorithm during inverter switching.

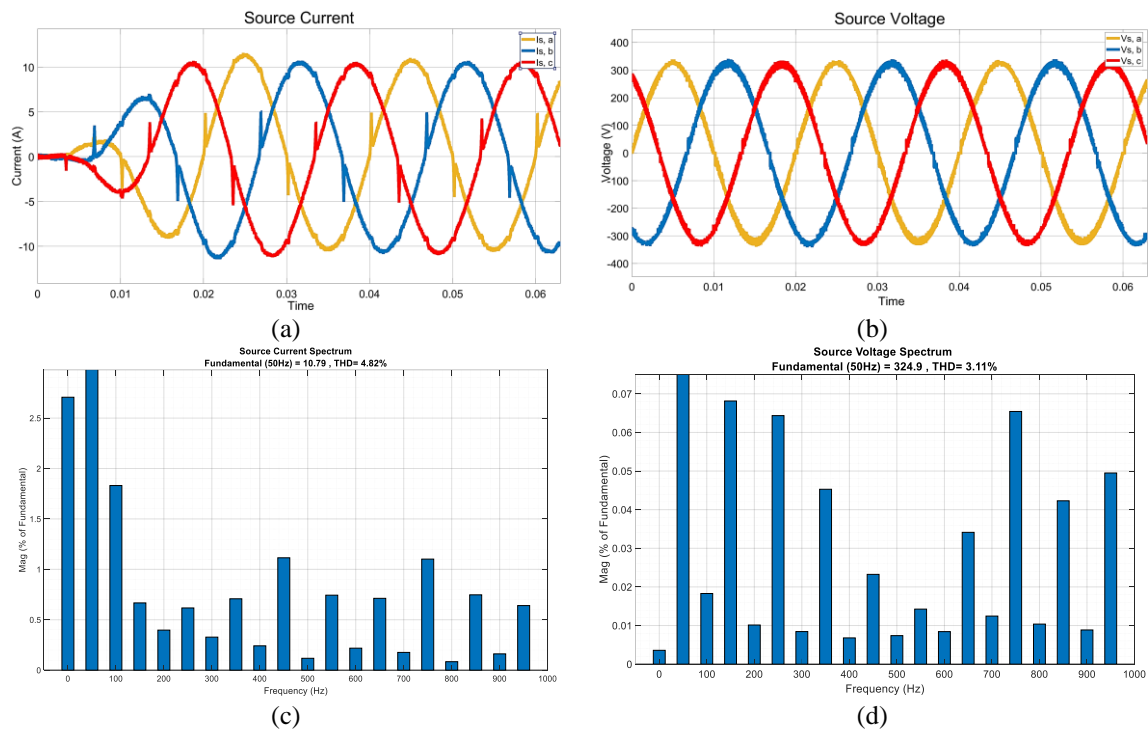


Figure 7. Source parameters: (a) source current wave, (b) source voltage wave, (c) THD source current, and (d) THD source voltage

### 3.2. Unbalanced load simulation

For the unbalanced load simulation with different load values per phase, the load resistance phase  $RL_a = 25 \, \Omega$  and inductance load phase  $LL_a = 70 \, \text{mH}$ , the phase b values are  $RL_b = 13 \, \Omega$  and  $LL_b = 60 \, \text{mH}$ , and for phase c,  $RL_c = 37 \, \Omega$  and  $LL_c = 50 \, \text{mH}$ . The simulation produced different currents for each phase: 7.96 A, 14.96 A, and 5.6 A for phases a, b, and c, respectively. The differences in amplitude across the load currents are illustrated in Figure 8(a), with phase b exhibiting the highest amplitude. However, as shown in Figure 8(b), the load voltage remained consistent across all the phases, indicating no significant variation despite the current amplitude differences. The THD of the load current varied significantly between phases, with phase b having the highest THD of 38.25%, corresponding to its larger current amplitude. The harmonic spectrum of the load current is depicted in Figure 8(c), which shows the frequency components contributing to the distortion. The voltage harmonic spectrum shown in Figure 8(d) indicates a relatively low THD of approximately 3% across all phases, with phase b slightly higher at 3.75%. This highlights the more pronounced harmonic distortion in the current compared with the voltage, which remains relatively stable and within acceptable limits.

The different load currents owing to imbalance, according to Figure 9(a), are transformed in the SRF to produce the current  $dq0$ , as shown in Figure 9(b). The ripples in the  $i_d$ ,  $i_q$ , and  $i_0$  currents were higher, indicating a load imbalance. The filtering of the  $dq0$  current to generate the reference current in  $dq0$  is depicted in Figure 9(c). Through Clarke retransformation, a reference current in the  $abc$  phase was obtained for the switching pattern, as shown in Figure 9(d).

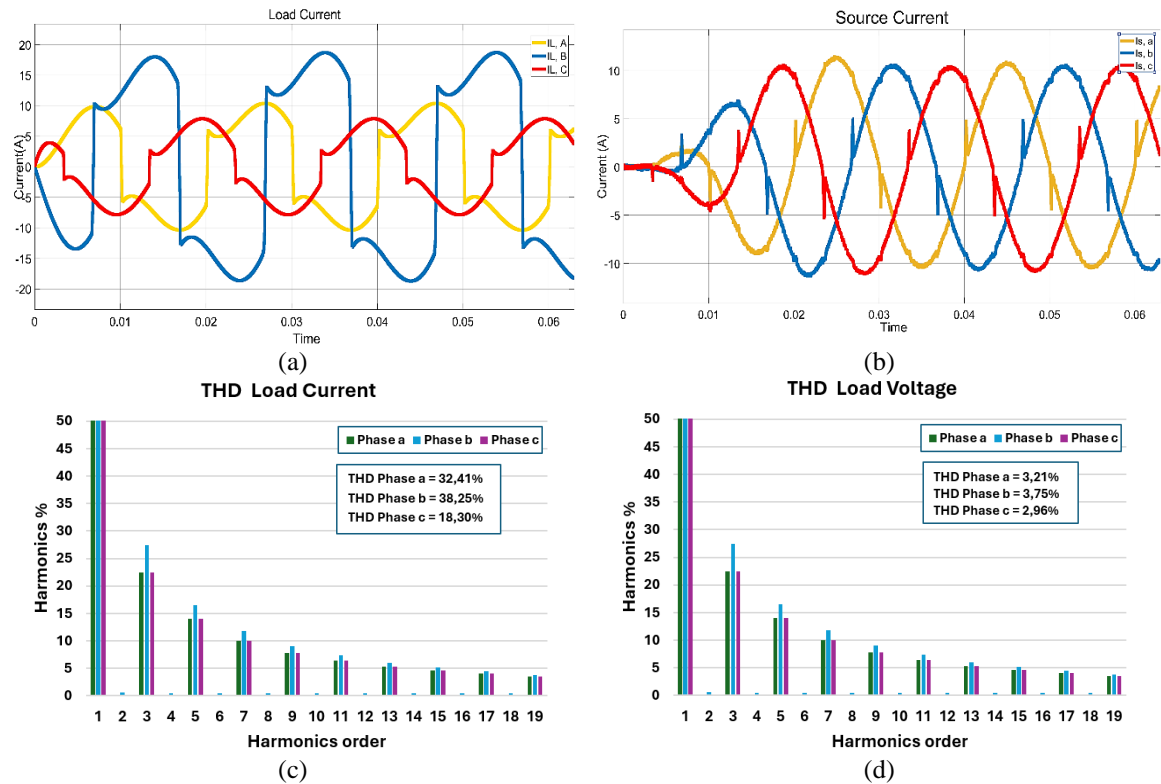


Figure 8. Load parameters: (a) load current wave per phase; (b) load voltage wave per phase; (c) THD load current phase a, b, and c; and (d) THD load voltage phase a, b, and c

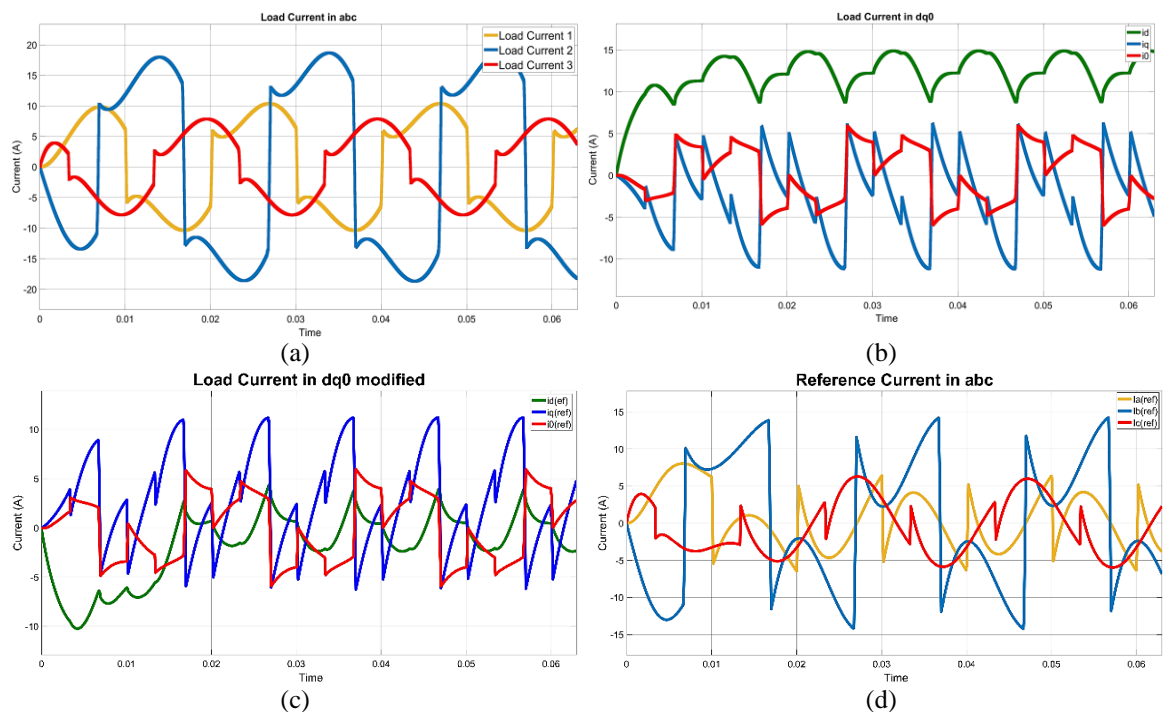


Figure 9. Current waveform: (a) load current in abc (b), load current in dq0, (c) reference current in dq0, and (d) reference current in abc

The inverter voltage connected to the PCC produces the source current, as shown in Figure 10(a). A significant balance of the phase current exists with minimal differences: phase a = 8.25 A, phase b = 8.27

A, and phase c = 8.47 A. On average, the voltage remained relatively stable at 230 V, as shown in Figure 10(b). In the harmonic spectrum of the current, the largest decrease occurred in phase c (2.90%), followed by phases a (4.54%) and b (14.44%). The high THD current of phase b is due to a spike anomaly in the algorithm. The THD current for each phase is shown in Figure 10(c). The harmonic spectrum THD voltage was approximately 3%, as shown in Figure 10(d). As a result of the load imbalance in variation 2, the neutral current increases to 10.71 amperes. After installation of the power filter, the neutral current decreases to 1.45 amperes due to load-balancing. The load current flowing to the source becomes balanced, thereby reducing the neutral current flowing to the source.

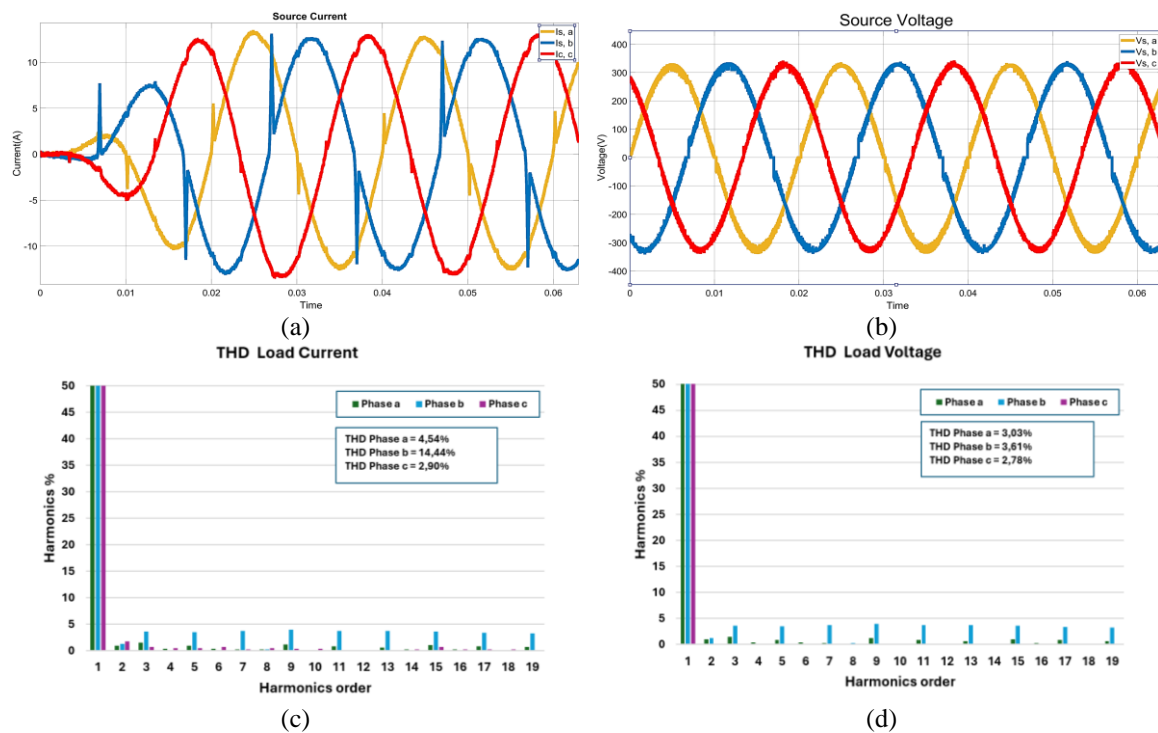


Figure 10. Source parameters: (a) source current waves per phase; (b) source voltage waves per phase; (c) THD source currents phases a, b, and c; and (d) THD load voltage phases a, b, and c

#### 4. CONCLUSION

This study successfully demonstrated the effectiveness of a hybrid power filter based on a five-level multilevel inverter controlled using MPC in mitigating harmonics and enhancing the power quality in three-phase, four-wire power grids. The proposed system reduced the THD to below 5%, met industry standards, and significantly minimized the neutral currents by up to one-tenth of their original values, even under dynamic and unbalanced load conditions. By integrating a passive LC filter with an active power filter, the solution provides robust load balancing, ensuring a stable and efficient operation. The adoption of MPC for optimal switching control proved to be highly effective, advancing its application in active power filter systems, which has been underexplored in previous research.

Future research could expand upon this work by exploring the application of hybrid power filters in other power system configurations, such as distributed generation or renewable energy sources. Investigating the integration of advanced reference current generation techniques, such as those leveraging artificial intelligence or machine learning, could further enhance harmonic compensation accuracy. Additionally, hardware implementation and real-world testing of the proposed system would validate its scalability, reliability, and adaptability to various operational conditions, providing a pathway for industrial adoption.

#### ACKNOWLEDGEMENTS

The author is grateful to the Indonesia Endowment Fund for Education Agency LPDP Ministry of Finance of the Republic of Indonesia through the National Research and Innovation Agency of BRIN

Indonesia for financing this research through the 2023-2024 Research and Innovation for Advanced Indonesia (RIIM) grant for the production of this article.

### FUNDING INFORMATION

This work was supported by Badan Riset dan Inovasi Nasional (BRIN) under Decree No. 37/II.7/HK/2023 from the Deputy of Research and Innovation Facilitation for the Research and Innovation Program for Advanced Indonesia, Batch 4 (*Program Riset dan Inovasi untuk Indonesia Maju Gelombang 4*).

### AUTHOR CONTRIBUTIONS STATEMENT

This journal uses the Contributor Roles Taxonomy (CRediT) to recognize individual author contributions, reduce authorship disputes, and facilitate collaboration.

Name of Author	C	M	So	Va	Fo	I	R	D	O	E	Vi	Su	P	Fu
Asep Andang	✓	✓	✓	✓	✓	✓		✓	✓	✓		✓		✓
Firmansyah Maulana Nursuwars			✓					✓		✓	✓			
Andri Ulus Rahayu			✓		✓		✓			✓		✓		
Imam Taufiqurrahman	✓	✓		✓					✓	✓			✓	
Ervan Paryono				✓		✓		✓	✓	✓	✓		✓	

C : Conceptualization

M : Methodology

So : Software

Va : Validation

Fo : Formal analysis

I : Investigation

R : Resources

D : Data Curation

O : Writing - Original Draft

E : Writing - Review & Editing

Vi : Visualization

Su : Supervision

P : Project administration

Fu : Funding acquisition

### CONFLICT OF INTEREST STATEMENT

Authors state no conflict of interest.

### DATA AVAILABILITY

The data supporting this study's findings are available from the corresponding author, [AA], upon reasonable request. These newly collected data can be shared as needed for research purposes.




### REFERENCES

- [1] B. K. Bose, *Power Electronics and Motor Drives: Advances and Trends*. Elsevier, 2021, doi: 10.1016/C2019-0-02032-8.
- [2] J. Rodriguez, F. Blaabjerg, and M. P. Kazmierkowski, "Energy transition technology: The role of power electronics," *Proceedings of the IEEE*, vol. 111, no. 4, pp. 329–334, Apr. 2023, doi: 10.1109/JPROC.2023.3257421.
- [3] J. G. Kassakian, D. J. Perreault, G. C. Verghese, and M. F. Schlecht, *Principles of Power Electronics*. Cambridge University Press, 2023, doi: 10.1017/9781009023894.
- [4] N. Mohan, *Power Electronics A first course, Simulations and Laboratory Implementations*, 2nd ed., no. 9. New Jersey: Wiley & Sons, Inc, 2023.
- [5] M. H. Nguyen and S. Kwak, "Enhance reliability of semiconductor devices in power converters," *Electronics*, vol. 9, no. 12, p. 2068, Dec. 2020, doi: 10.3390/electronics9122068.
- [6] K. R. Shandilya and U. S. Patel, "Mitigation of total harmonic distortion using cascaded MLI-DSTATCOM in distribution network," in *2017 IEEE International Conference on Power, Control, Signals and Instrumentation Engineering (ICPCSII)*, IEEE, Sep. 2017, pp. 2439–2445, doi: 10.1109/ICPCSII.2017.8392155.
- [7] J. C. Das, *Power System Harmonics and Passive Filter Designs*. Wiley-IEEE Press, 2015, doi: 10.1002/9781118887059.
- [8] D. Lumbreras, E. Gálvez, A. Collado, and J. Zaragoza, "Trends in power quality, harmonic mitigation and standards for light and heavy industries: A review," *Energies*, vol. 13, no. 21, p. 5792, Nov. 2020, doi: 10.3390/en13215792.
- [9] D. Pejovski, K. Najdenkoski, and M. Dugalovski, "Impact of different harmonic loads on distribution transformers," *Procedia Engineering*, vol. 202, pp. 76–87, 2017, doi: 10.1016/j.proeng.2017.09.696.
- [10] A. Kalair, N. Abas, A. R. Kalair, Z. Saleem, and N. Khan, "Review of harmonic analysis, modeling and mitigation techniques," *Renewable and Sustainable Energy Reviews*, vol. 78, pp. 1152–1187, Oct. 2017, doi: 10.1016/j.rser.2017.04.121.
- [11] H. G. Beleiu, V. Maier, S. G. Pavel, I. Birou, C. S. Pică, and P. C. Dărab, "Harmonics consequences on drive systems with induction motor," *Applied Sciences*, vol. 10, no. 4, p. 1528, Feb. 2020, doi: 10.3390/app10041528.
- [12] Y. Tanaka, T. Tajima, M. Seyama, and K. Waki, "Differential continuous wave photoacoustic spectroscopy for non-invasive glucose monitoring," *IEEE Sensors Journal*, vol. 20, no. 8, pp. 4453–4458, Apr. 2020, doi: 10.1109/JSEN.2019.2962251.
- [13] A. Benjamin and S. K. Jain, "A review of literature on effects of harmonics on protective relays," in *2018 IEEE Innovative Smart Grid Technologies - Asia (ISGT Asia)*, IEEE, May 2018, pp. 407–412, doi: 10.1109/ISGT-Asia.2018.8467876.
- [14] F. Zare, H. Soltani, D. Kumar, P. Davari, H. A. M. Delpino, and F. Blaabjerg, "Harmonic emissions of three-phase diode rectifiers in distribution networks," *IEEE Access*, vol. 5, pp. 2819–2833, 2017, doi: 10.1109/ACCESS.2017.2669578.

- [15] B. Singh, A. Chandra, and K. Al-Haddad, *Power Quality Problems and Mitigation Techniques*, vol. 9781118922057. Wiley, 2015, doi: 10.1002/9781118922064.
- [16] C.-S. Lam and M.-C. Wong, *Design and control of hybrid active power filters*. in SpringerBriefs in Electrical and Computer Engineering. Berlin, Heidelberg: Springer Berlin Heidelberg, 2014, doi: 10.1007/978-3-642-41323-0.
- [17] M. H. Rashid, *Power Electronics Handbook*, Elsevier, 2017.
- [18] R. Chander, E. V. S. Rao, and E. V. Sagar, "Adjustable step-size LMS based IRP method for active power filter," in *2020 International Conference on Computer Communication and Informatics (ICCCI)*, IEEE, Jan. 2020, pp. 1–6, doi: 10.1109/ICCCI48352.2020.9104127.
- [19] S. F. Al-Gahtani and R. M. Nelms, "A frequency adaptive control scheme for a three-phase shunt active power filter," *Electrical Engineering*, vol. 103, no. 1, pp. 595–606, Feb. 2021, doi: 10.1007/s00202-020-01105-4.
- [20] A. Andang, R. S. Sarkar, S. Mukherjee, T. Pal, and I. N. S. Kumara, "Grid-connected inverter using model predictive control to reduce harmonics in three-phase four-wires distribution system," *Engineering Letters*, vol. 30, no. 1, pp. 108–116, 2022.
- [21] K. M. Abdulhassan and O. Y. K. Al-Atbee, "Improved modified a multi-level inverter with a minimum total harmonic distortion," *Bulletin of Electrical Engineering and Informatics*, vol. 11, no. 2, pp. 672–680, Apr. 2022, doi: 10.11591/eei.v11i2.3466.
- [22] G. Ghosh, S. Sarkar, S. Mukherjee, T. Pal, and S. Sen, "A comparative study of different multilevel inverters," *2017 1st International Conference on Electronics, Materials Engineering and Nano-Technology, IEMENTech 2017*, 2017, doi: 10.1109/IEMENTECH.2017.8076971.
- [23] N. Kavitha and J. F. Roseline, "Neural network-based fault classification in multi-level inverters," *ICSPC 2023 - 4th International Conference on Signal Processing and Communication*, 2023, pp. 123–127, doi: 10.1109/ICSPC57692.2023.10126047.
- [24] O. M. H. Anssari, M. Badamchizadeh, and S. Ghaemi, "Designing of a PSO-based adaptive SMC with a multilevel inverter for MPPT of PV systems under rapidly changing weather conditions," *IEEE Access*, vol. 12, pp. 41421–41435, 2024, doi: 10.1109/ACCESS.2024.3377925.
- [25] E. Sundaram, M. Gunasekaran, R. Krishnan, S. Padmanaban, S. Chenniappan, and A. H. Ertas, "Genetic algorithm based reference current control extraction based shunt active power filter," *International Transactions on Electrical Energy Systems*, vol. 31, no. 1, 2021, doi: 10.1002/2050-7038.12623.
- [26] S. Saad and L. Zellouma, "Fuzzy logic controller for three-level shunt active filter compensating harmonics and reactive power," *Electric Power Systems Research*, vol. 79, no. 10, pp. 1337–1341, Oct. 2009, doi: 10.1016/j.epsr.2009.04.003.
- [27] M. S. Badra, S. Barkat, and M. Bouzidi, "Backstepping control of three-phase three-level four-leg shunt active power filter," *Journal of Fundamental and Applied Sciences*, vol. 9, no. 1, p. 274, 2017, doi: 10.4314/jfas.v9i1.18.
- [28] J. L. Monroy-Morales, D. Campos-Gaona, M. Hernández-Ángeles, R. Peña-Alzola, and J. L. Guardado-Zavala, "An active power filter based on a three-level inverter and 3D-SVPWM for selective harmonic and reactive compensation," *Energies*, vol. 10, no. 3, 2017, doi: 10.3390/en10030297.
- [29] M. Mehra, E. Pouresmaeil, M. F. Akorede, B. N. Jørgensen, and J. P. S. Catalão, "Multilevel converter control approach of active power filter for harmonics elimination in electric grids," *Energy*, vol. 84, pp. 722–731, 2015, doi: 10.1016/j.energy.2015.03.038.
- [30] U. Gajula, "Reduced switch multilevel inverter based shunt active power filter with ANN controller for power quality improvement," *Journal of Electrical Systems*, vol. 20, no. 3, pp. 641–650, 2024, doi: 10.52783/jes.2990.
- [31] G. Krithiga and V. Mohan, "Elimination of harmonics in multilevel inverter using multi-group marine predator algorithm-based enhanced RNN," *International Transactions on Electrical Energy Systems*, vol. 2022, 2022, doi: 10.1155/2022/8004425.
- [32] P. K. Dash, E. N. V. D. V. Prasad, R. K. Jalli, and S. P. Mishra, "Multiple power quality disturbances analysis in photovoltaic integrated direct current microgrid using adaptive morphological filter with deep learning algorithm," *Applied Energy*, vol. 309, 2022, doi: 10.1016/j.apenergy.2021.118454.
- [33] A. Kumar and S. Jain, "Predictive switching control for multilevel inverter using CNN-LSTM for voltage regulation," *ADB U Journal of Engineering Technology*, vol. 11, pp. 2348–7305, 2022.
- [34] A. Sahli, F. Krim, A. Laib, and B. Talbi, "Model predictive control for single phase active power filter using modified packed U-cell (MPUC5) converter," *Electric Power Systems Research*, vol. 180, 2020, doi: 10.1016/j.epsr.2019.106139.
- [35] M. Adam, Y. Chen, and X. Deng, "Harmonic current compensation using active power filter based on model predictive control technology," *Journal of Power Electronics*, vol. 18, no. 6, pp. 1889–1900, 2018, doi: 10.6113/JPE.2018.18.6.1889.
- [36] E. Skjong, T. A. Johansen, and M. Molinas, "Distributed control architecture for real-time model predictive control for system-level harmonic mitigation in power systems," *ISA Transactions*, vol. 93, pp. 231–243, 2019, doi: 10.1016/j.isatra.2019.01.043.
- [37] V. Yaramasu, M. Rivera, A. Dekka, and J. Rodriguez, "Predictive control of four-leg converters for photovoltaic energy systems," *Power Systems*, pp. 45–69, 2019, doi: 10.1007/978-981-13-6151-7\_3.




## BIOGRAPHIES OF AUTHORS






**Asep Andang**    has been a lecturer in the Electrical Engineering Department at Universitas Siliwangi Tasikmalaya, Indonesia, since 2001. He received a B.Eng. degree in Electrical Engineering from Universitas Siliwangi in 2000, received an M.Eng. degree in Electrical Engineering from Institut Teknologi of Bandung in 2006, and received a Ph.D. degree in Engineering Science from Universitas Udayana Bali in 2021. He became a member of IEEE in 2020. He has been an associate professor with Universitas Siliwangi since 2021. His research interests are in power quality, power electronics and drive, industrial control and automation, the internet of things, and electromedicine. He can be contacted at email: andhangs@unsil.ac.id.








**Firmansyah Maulana Nursuwars**    was born in Tasikmalaya on December 05, 1983. He has been a lecturer in the informatics department at Universitas Siliwangi Tasikmalaya, Indonesia, since 2009. He received a B.Eng. degree in Electrical Engineering from Universitas Siliwangi in 2006 and received an M.Com. degree in STMIK Likmi Bandung in 2015. His research interests are in control and automation, the internet of things, and smart systems. He can be contacted at email: firmansyah@unsil.ac.id.






**Andri Ulus Rahayu**    was born in Bandung on April 03, 1989. He is currently serving as a lecturer at the Department of Electrical Engineering at Universitas Siliwangi. His current research interests are in the field of control systems based on computer technology and IoT. He can be contacted at email: andriulusr@unsil.ac.id.



**Imam Taufiqurrahman**    was born in Bandung, June 12, 1990. He holds a bachelor's degree in Electronic Engineering Education at the University of Education Indonesia (UPI) and a master's degree in Electrical Engineering at the Bandung Institute of Technology (ITB). Currently, he is serving as a lecturer at the Department of Electrical Engineering at Universitas Siliwangi. The research fields currently pursued are control systems, automation, robotics, and intelligent systems. He can be contacted at email: imamtaufiqurrahman@unsil.ac.id.



**Ervan Paryono**    earned his bachelor's degree in Electrical Engineering in 2022 at Universitas Siliwangi, Indonesia. He is enthusiastic about power electronics, embedded systems, drive systems, and control systems. He can be contacted at email: paryonoervan@gmail.com.